Pol. J. Environ. Stud. Vol. 22, No. 5 (2013), 1363-1370

Original Research

Adsorption of Disperse of Yellow 42 onto Bentonite and Organo-Modified Bentonite by Tetra Butyl Ammonium Iodide (B-TBAI)

Saeedeh Hashemian*, Bahareh Sadeghi, Fatemeh Mozafari, Hamila Salehifar, Khatereh Salari

Chemistry Department, Yazd Brunch, Islamic Azad University, Yazd, Iran

Received: 23 September 2012
Accepted: 8 January 2013

Abstract

The kinetics and thermodynamics of adsorption of disperse yellow (DY42) by bentonite and organo-modified-bentonite was studied. The organo-modified bentonite was synthesized by bentonite and tetra butyl ammonium iodide (B/TBAI). The B/TBAI was characterized by FT-IR, XRD, SEM, and elemental analysis. The adsorption experiments were carried out to investigate the factors that influence dye uptake by the adsorbents, such as the contact time under agitation, adsorbent dosage, initial dye concentration, and pH. The experimental results show that the percentage of dye removal increases with the increasing the amount of sorbent. Adsorption was pH-dependent. The equilibrium data were fitted to Langmuir and Freundlich isotherms and the equilibrium adsorption was best described by the Langmuir isotherm model. The experimental data fitted very well with the pseudo-first-order kinetic model. The thermodynamic study of the adsorption process showed that the adsorption of DY42 onto B-TBAI adsorbent was carried out spontaneously and the process was endothermic in nature.

Keywords: adsorption, bentonite, disperse yellow 42, organo-bentonite

Introduction

Disperse dyes are widely used in a variety of industries such as textiles, paper, and leather. Disperse dyes were originally developed for the dyeing of cellulose acetate and are water insoluble. Disperse dyes are non-ionic aromatic compounds, scarcely soluble in water but soluble in organic solvent [1]. Textile industry effluent contains many dyes that include carcinogenic and mutagenic chemicals such as benzidine, metals, etc., and causes serious environmental problems. Dyes are visible even at low concentrations and are difficult to biodegrade in the environment due to their resistance to light, heat, chemicals, and water [2]. In this manner, these kinds of pollutants must be treated prior to their discharge into the receiving water bodies.

*e-mail: Sa_hashemian@yahoo.com

The conventional treatments of dyed wastewater include chemical coagulation, biological and electrochemical processes, ozonation, and adsorption [3-11]. Adsorption onto activated carbon has been proven to be an effective process for dye removal, but it is expensive. This has largely been associated with the cost of producing activated carbon, and the lack of suitable and inexpensive regeneration procedures for these adsorbents. In recent years, there has been growing interest in finding inexpensive and effective adsorbents such as fly ash [12], peat [13], wood powder [14], sawdust composite [15], coir pith [16], and lignin [17]. Bentonite is primarily expandable montmorillonite clay. Montmorrllonite is a 2:1 type of mineral, and its unit layer structure consists of one Al^{+3} octahedral sheets [18]. Basically, the modification reactions are accomplished by replacing the inter layer cations (e.g. Na^{+}, K^{+}, Ca^{2+}) with specific species to alter the surface and structural characteristics

of the clay. Hence organo clays are powerful adsorbents for a wide variety of environmental applications [19-28]. The surface properties of bentonite can be greatly modified with a surfactant by simple ion-exchange reactions. This is favoured by Vanderwaals interaction between organic surfactant cations and the reduced solvent shielding of the ions in the interamolecular environment. Large organic cations (cationic surfactants) of the form $(CH_3)_3N^+$ R (where R is an alkyl hydrocarbon) occupy the exchange sites of the bentonite clay and hence the surface area is increased.

In this study, organo-modified-bentonite (B-TBAI) was prepared and characterized. Adsorption behavior of DY42 dye on B-TBAI was studied. Optimum conditions for adsorption of DY42 were determined. Also, in order to evaluate the adsorption process we used the first- and second-order sorption kinetics model. The Langmuir and Freundlich isotherms were investigated.

Experimental

Material and Methods

Disperse yellow 42 (DY42) (4-anilino-3-nitro-N-phenylbenzenesulphonamide) with C.I. 10338 was obtained from Merck and was used without further purification. The dye has molecular formula $C_{18}H_{15}N_3O_4S$ and molecular weight 369.3944. The standard dye solution of 1,000 mg·L^{-1} was prepared as stock solution and subsequently, whenever necessary, diluted. The chemical structure of DY42 is shown in Fig. 1. All chemicals and reagents were of analytical grade and from Merck.

Bentonite was used as an adsorbent (particle size fractions of 106-200 μm) and obtained from tavan sil co of Iran. It was crushed and dried at 120ºC in an oven for 5 h prior to use. The cation exchange capacity (CEC) and surface area determined by the methylen blue method were 650 mmol·kg^{-1} and 450 m^2·g^{-1}, respectively [29].

Tetra butyl ammonium iodide (TBAI) as organo-modification was obtained from Merck.

Synthesis of Organo-Bentonite (B-TBAI)

The preparation process was carried out by dispersing l0 g bentonite to a 100 mL of TBAI 1 mol·L^{-1}. The mixture was shacked for 3 h at room temperature. The bentonite loaded with TBAI was filtered, washed repeatedly with copious amounts of distilled water, then dried in air and stored for subsequent studies [28].

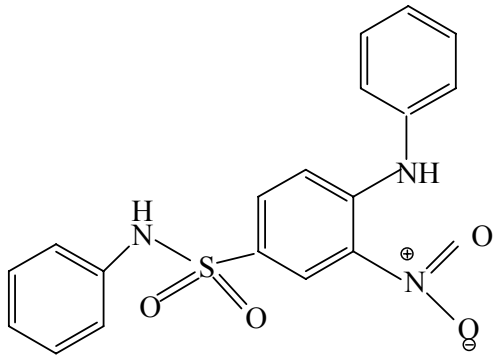

Fig. 1. Chemical structure of DY42.

Adsorption Studies

In order to study the effects of different parameters such as the contact time, pH, sorbent dosage, and initial dye concentration on sorption, various experiments have been carried out by agitation of known amounts of B-TBAI (0.1 g) in 50 mL of dye solution with an initial concentration of 100 mg·L^{-1} on a rotary shaker at a constant speed of 150 rpm at room temperature (25ºC). Samples were withdrawn at appropriate time intervals and centrifuged at 3,000 rpm for 5 min, and the absorbance of the supernatant was measured using a UV-vis spectrophotometer at maximum absorbance (λ_{max}) of dye. The effect of pH was studied by adjusting the pH of the dye solutions in the range of 2-12 with 0.1 N NaOH or HCl solutions. To evaluate the adsorption thermodynamic parameters, the effects of temperature on adsorption were carried out at 20-60ºC. Kinetics of adsorption were determined by analyzing sorbate uptake of the dye from aqueous solution at different time intervals. For sorption isotherm determination, dye solutions of different concentrations were agitated with known amounts of sorbents until the equilibrium was achieved at room temperature (25ºC). The amount of DY42 adsorbed by sorbent % adsorption was calculated by the following mass balance relationship:

$$\%Adsorption = (C_0\text{-}C) / C_0 \times 100$$

...where C_0 and C (mg·L^{-1}) are the initial and equilibrium solution concentrations of DY42, respectively.

Characterization Method

The obtained products were characterized by FT-IR (tensor-27 of Burker) using the KBr pellet. X-ray diffraction (XRD) measurements were carried out with a D8 Bruker. The X-ray diffractometer was equipped with a monochromator in a 2θ range of 5-70˚ using a cu k_α radiation source accelerated at 40KV and 30 mA .The percentage of C, H, and N in the free and surfactant-loaded bentonite were determined by a CHN elemental analyzer Costech-ECS-4010. A UV-vis spectrophotometer 160 A Shimadzu was used for determining dye concentration. All pH measurements were carried out with an ISTEK- 720P pH meter. Scanning electron microscopy was performed using a Philips SEM 501 electron microscope. The specific BET surface area was measured at 77K (Quanta chrome, Autosorb-1).

Results and Discussion

Characterization of Sorbent

The bentonite and prepared organ-clay (B-TBAI) were characterized with FT-IR, XRD, and SEM. FT-IR spectrum of bentonite showed peaks at 3,629, 3,440, and 1,040 cm^{-1}

(Fig. 2). The absorption band at 3,629 cm^{-1} is due to stretching vibrations of structural OH groups of monmorillonite. Water in montmorillonite gave a broad and shoulder bound near 3,440 cm^{-1}, corresponding to the H_2O stretching vibrations [30]. A complex band at 1,040 cm^{-1} is related to the stretching vibrations of Si-O groups, while the bands at 518 and 465 cm^{-1} are due to Al-O-Si and Si-O-Si bending vibrations, respectively. The spectrum of the TBAI displayed two split peaks at 2,954 and 2,871 cm^{-1} that are assigned to the aliphatic C-H stretching vibration. The FT-IR spectrum of B-TBAI was characterized by the appearance of above characteristic peaks. These results indicate the existence of the TBAI on the modified bentonite.

The XRD pattern of bentonite showed the characteristic reflections of montmorillonite at 7.2˚, 20˚, 28˚, 22˚, and those of quartz at 21-26˚ 2θ [30]. Fig. 3 shows the X-ray diffraction patterns of bentonite, TBAI and B/TBAI/DY42. The reflections at 2θ = 9.3 and 22.5 are characteristic of TBAI. The XRD and FT-IR spectra of bentonite indicate that montmorillonite is the dominant mineral phase in this clay (Figs. 2 and 3). The XRD patterns of B-TBAI shows reflections characteristic for both bentonite and TBAI, but at lower intensity, which clearly indicates the presence of free surfactant that has not been removed by washing.

The specific surface area (BET) of B and B-TBAI was 32.5 and 10.7 m^2/g, respectively. The surface area of raw bentonite decreases upon modification. The decrease of the specific surface area may be attributed to the blocking of the porous aggregates and increase the aggregation of particles. Decreasing the surface area of bentonite with increasing degrees of modification is consistent with the results of previous studies [31, 32].

The content of C, H, and N in B-TBAI was increased by the modification of TBAI on the bentonite surface. In particular, the presence of nitrogen in the B-TBAI confirms the presence of TBAI onto bentonite. The C/N ratio of B-TBAI was closed to the theoretical C/N ratios (Table 1).

The morphologies of B, TBAI, B-TBAI, and B-TBAI loaded DY42, were studied by SEM. SEM micrograph of a-B, b-TBAI, c-B-TBAI, and d-B-TBAI loaded DY42 are shown in Fig. 4. It can be observed that the particles of bentonite have different shapes and sizes (Fig 4-a). The B-TBAI particles have small size with uniform shape (Fig 4-c) suitable for adsorption.

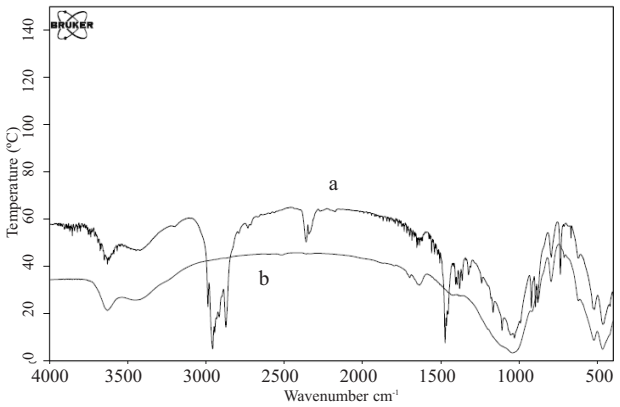

Fig. 2. FTIR of a) a-B-TBAI b) bentonite.

Table 1. Elemental analysis and C/N of bentonite and RB-TBAI.

Phase	Elemental analysis (W %)			C/N ratio
	C (*)	H (*)	N (*)	
Bentonite	1.3 (0)	0.7 (0.8)	0 (0)	-
TBAI	53.0 (52.0)	10.3 (9)	3.7 (3.0)	14.32 (17.33)
B-TBAI	34.1 (23)	0.7 (4)	2.5 (1.71)	13.64 (13.45)

*Calculated

Effect of Contact Time

The effect of contact time on removal of DY42 by B and B-TBAI is shown in Fig. 5. The dye adsorption by B-TBAI sorbent is faster than that of bentonite. The rate of adsorption is initially quite rapid, with most of the compound being adsorbed within the first few minutes. The rate of adsorption then slows down with the elapsed time until an apparent equilibrium is reached. As seen from Fig. 5, that equilibrium time required for the adsorption of DY42 is almost 60 min. TBAI modification covered the bentonite

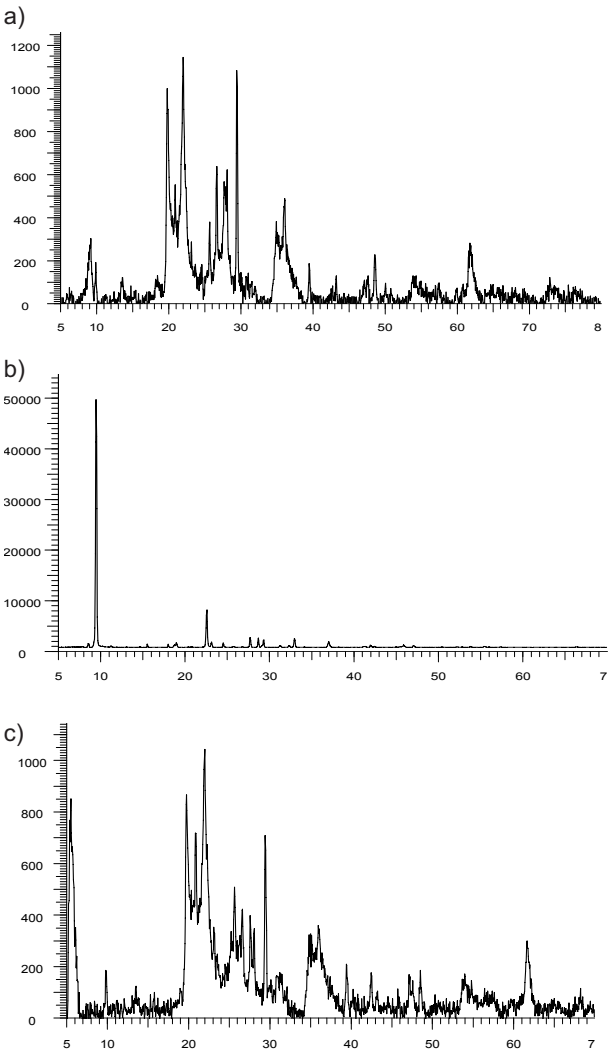

Fig. 3. XRD patterns of a-B, b-TBAI, c-B/TBAI.

surfaces and increased molecular interaction between DY42 molecules. Therefore, uptake of dyes increased from bentonite to B-TBAI. After the equilibrium time, the increasing rate of adsorption of dye decreased and the amount of dye adsorbed remained almost the same. The removal of DY42 from aqueous solutions by modified bentonite seems to be more effective than in the unmodified sample.

The UV spectra of DY42 and DY42 loaded B-TBAI was studied. The spectrum is show in Fig. 6, which shows that there is a major absorbance peak at 416 nm in the visible spectra of DY42. This absorbance peak decreased in intensity as treatment time increased, and after treatment for 240 min this peak almost totally disappeared, which indicates the dye diminished after adsorption.

Effect of pH

The effect of pH on adsorption of DY42 on B-TBAI was studied by varying the pH of solution from 2 to 12. The experiments were carried out for 50 ml of dye 100 mg·L^{-1} and 0.5 g of sorbents for 60 min contact time. It was observed that pH gives a significant influence to the adsorption process [9, 10]. The adsorption percentage of DY42 with B-TBAI is increased with increasing pH value, and the maximum uptake of the dyes takes place at around pH 12 (Fig. 7). Adsorption of DY42 at higher pH is higher and it may be explained on the assumption that TBAI modification covered the clay surfaces with positive charges and increased electrochemical interaction between dye molecules and modified clay surfaces. The high Adsorption capacity is due to the strong electrostatic interaction between $-N^{+}(CH_3)_3$ of B-TBAI and dye. In contrast, betonite contains fewer adsorption sites, so a lower adsorption capacity was obtained due to the lack of electrostatic interaction between dye and bentonite [19]. Therefore, it is observed that the rate of removal of dyes increases with increased in pH for bentonite remaining constant and the percentage of dye removal is very low.

Effect of Initial Dye Concentration

The adsorption experiments were carried out in the concentration range of dye from 10-70 mg·L^{-1} at 0.5 g sorbent, contact time 60 min, and pH 12. As shown in Fig. 8, when the initial dye concentration was increased to 15 mg·L^{-1}, the adsorption uptake of dye increased to 94% for DY42, and at higher concentration the uptake is constant. These indicate that the initial dye concentrations play an important role in the adsorption of DY42 on the B-TBAI [33].

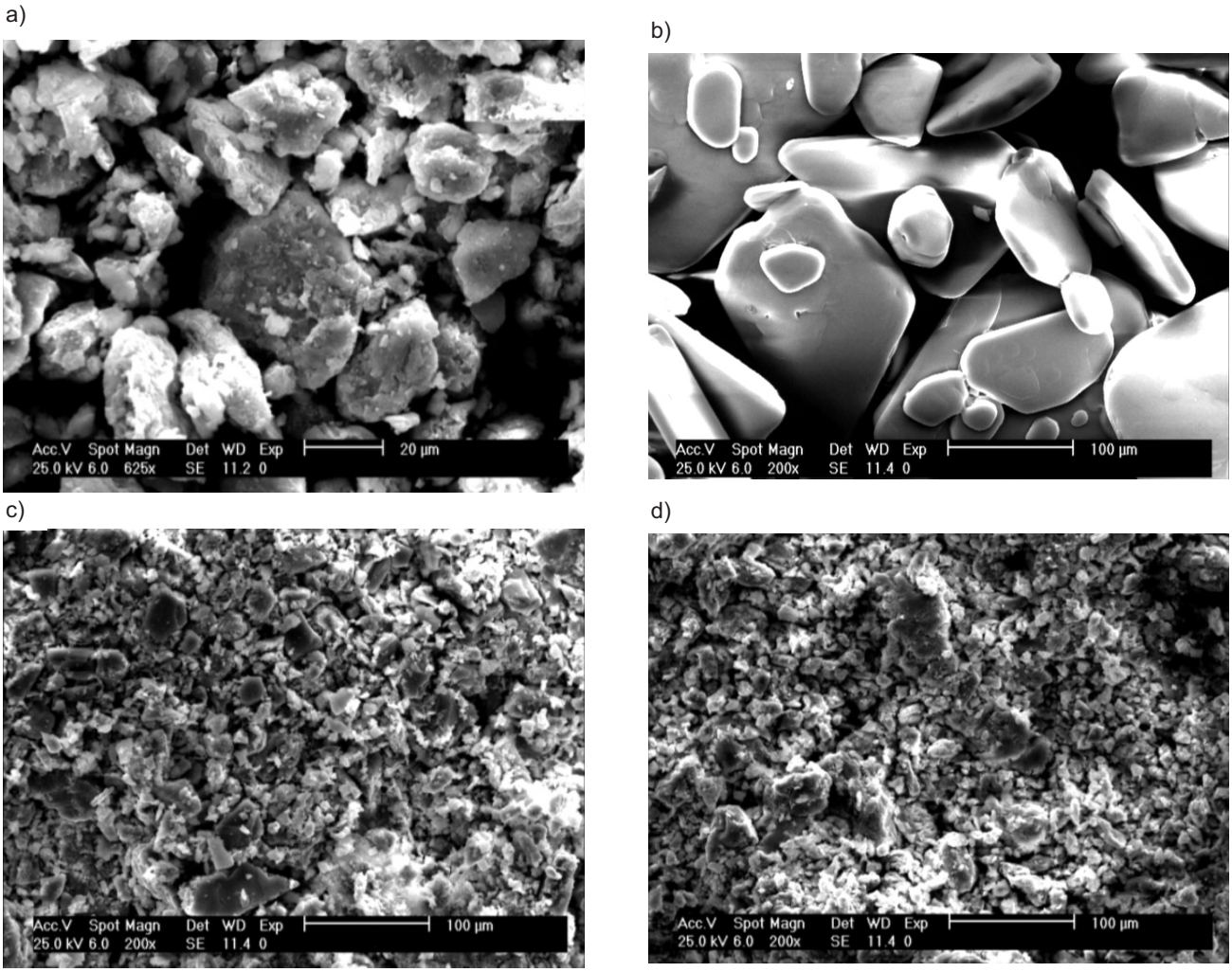

Fig. 4. SEM micrograph of a-B, b-TBAI, c-B/TBAI, and d- B/TBAI/DY42.

Effect of Adsorbent Dose

The effect of the adsorbent dose on the removal of DY42 was studied by varying the amount of adsorbent B-TBAI. Fig. 9 shows the removal of DY42 by B-TBAI at different adsorbent doses (0.1-1 g) for the volume of 50 mL at dye concentration 100 mg·L^{-1}. The results, in Fig. 9, clearly show an increase in adsorption with increases in the amount of adsorbents. An increase in adsorption with the adsorbent dosage can be attributed to the availability of more adsorption sites and greater surface area for contact. At m>0.2 g, the incremental DY42 uptake is very small as the DY42 surface concentration and the DY42 bulk solution concentration come to equilibrium with each other [11, 33].

Adsorption Kinetics

It is important to be able to predict the rate at which contamination is removed from the aqueous solution in order to design an adsorption treatment plant. The transient behavior of the dye adsorption process was analyzed using the pseudo-first and pseudo-second kinetic models.

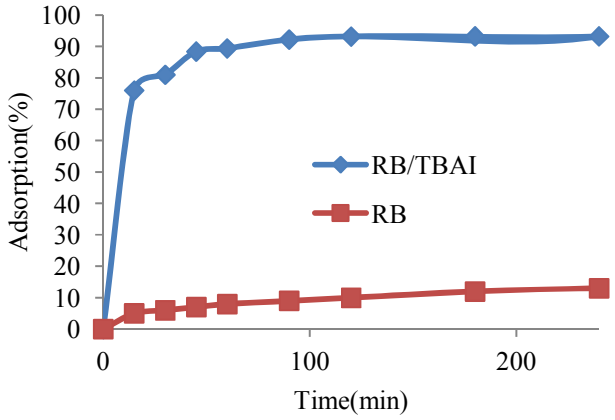

Fig. 5. Effect of contact time on the sorption of DY42. (50 ml of 100 mg·L^{-1} of DY42, pH 12, 0.5 g sorbent at room temperature).

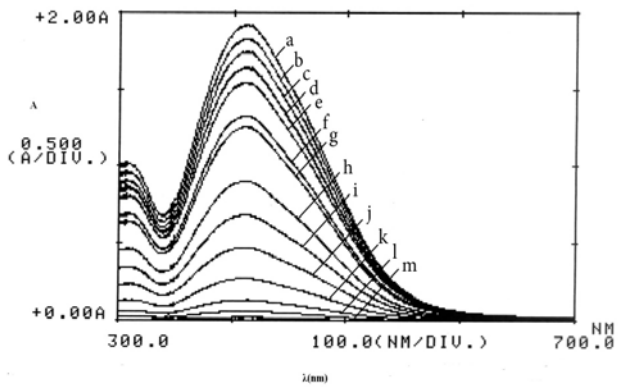

Fig. 6. UV-Vis electronic spectra of DY42 before and after adsorption at different times after: a – 0, b – 10 min, c – 20 min d – 30 min, e – 40 min, f – 50 min, g – 60 min, h – 75min, i – 90 min, j – 105 min, k – 120 min, l – 180 min, and m – 240 min (50 ml DY42 solution, initial concentration 100 mg·L^{-1}, initial pH 12.0, 0.1 g adsorbent B/TBAI).

The pseudo-first-order kinetic model was appropriate for lower concentration, with the equation expressed as follows [34]:

$$\mathrm{Ln}(q_e - q_t) = \mathrm{Ln}\, q_e - k_1 t \quad (1)$$

The rate of pseudo-second-order reaction depends on the amount of adsorbed solution, the surface of adsorbent,

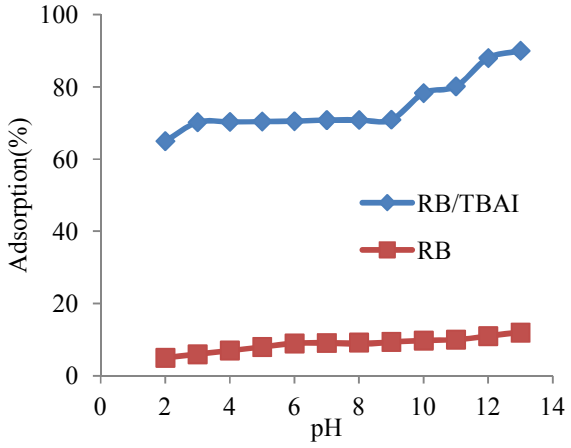

Fig. 7. Effect of pH for adsorption DY42 onto B-TBAI. (50 ml of 100 mg·L^{-1} of DY42 and 0.5 g sorbent at room temperature).

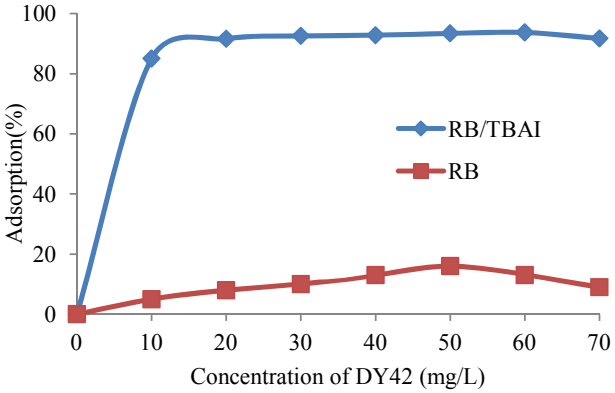

Fig. 8. Effect of dye concentration for adsorption DY42 onto B-TBAI. (50 ml of DY42 and 0.5 g sorbent at room temperature).

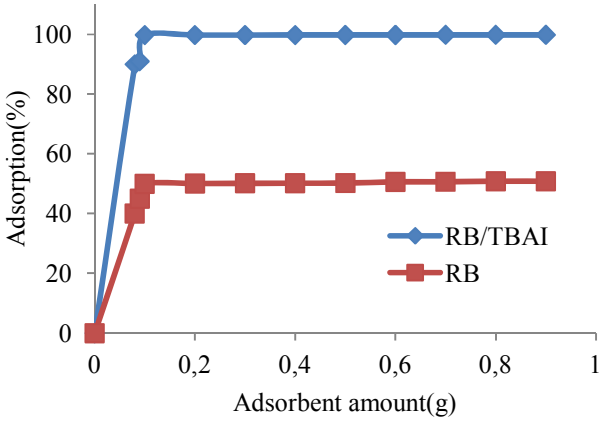

Fig. 9. Effect of amount of B-TBAI and bentonite on the adsorption of DY42.

Table 2. Kinetics parameters for the removal of DY42.

First order		Second order	
R^2	K_1	R^2	K_2
0.947	0.516	0.997	0.40

and the amount of adsorption at the equilibrium. The model was represented in the following linear form [13, 35]:

$$t/q_t = 1/kq_e^2 + t/q_e \quad (2)$$

...where q_t is the amount of dye adsorbed at time t (mg/g), q_e is the adsorption capacity at equilibrium (mg/g), and k_1 and k_2 are the apparent rate constants.

During this study, the two adsorption kinetic pseudo-first- and second-order models were used. The kinetics of pseudo-first-order and pseudo-second-order are discussed in Figs. 10 and 11. The related parameters are shown in Table 2. As shown, the R^2 value of the pseudo-second-order model is better fitted and the adsorption process follows pseudo-second older kinetics.

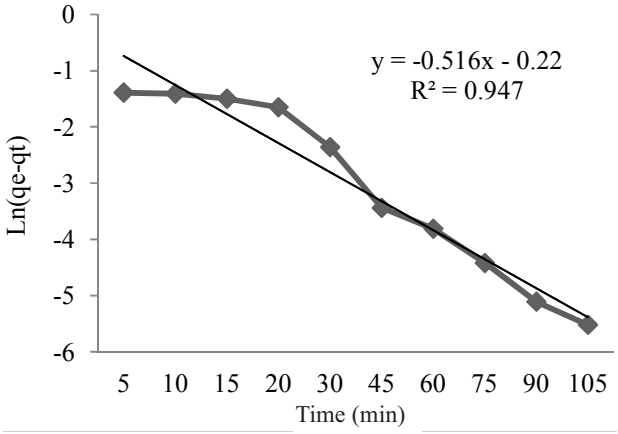

Fig. 10. Kinetic of pseudo-first-order model for adsorption of DY42 onto B-TBAI. (50 ml of initial concentration 100 mg·L^{-1}, pH 12, 0.5 g adsorbent).

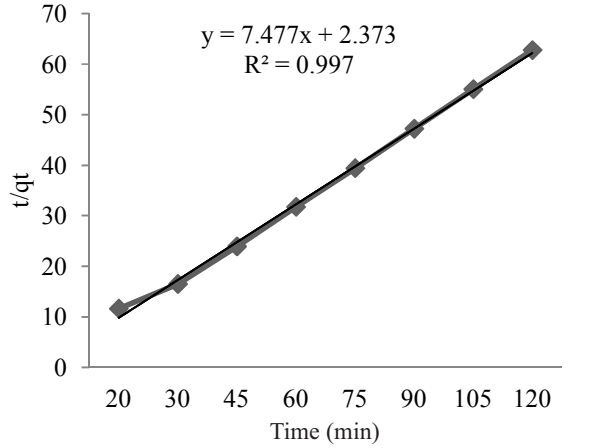

Fig. 11. Kinetic of pseudo-second-order model for adsorption of DY42 onto B-TBAI. (Initial concentration 100 mg·L^{-1}, pH 12, 0.5 g adsorbent).

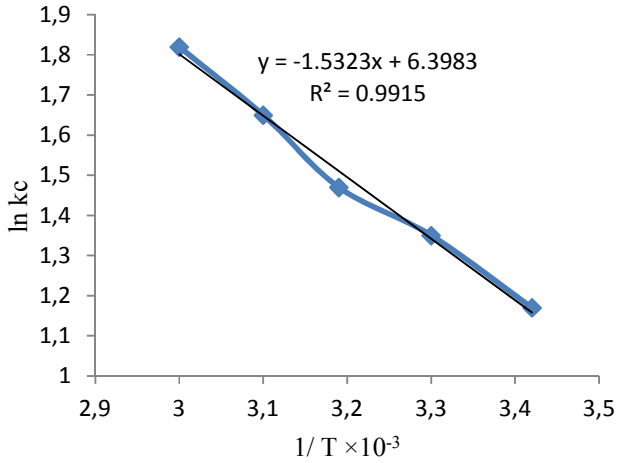

Fig. 12. Plot of ln Kc verses 1/T for adsorption DY42 onto B/TBAI.

Adsorption Isotherm of DY42

The adsorption isotherm indicates how the adsorption molecules are distributed between the liquid phase and the solid phase when the adsorption process reaches an equilibrium state.

The Langmuir adsorption model is given as:

$$q_e = q_m K_L C_e/(1+ K_L C_e) \quad (3)$$

The linearized form of Langmuir can be written as follows:

$$C_e/q_e = 1/q_m K_L + C_e/q_m \quad (4)$$

...where q_e is the solid-phase equilibrium concentration (mg·g^{-1}), C_e is the liquid equilibrium concentration of dye in solution (mg·L^{-1}), K_L is the equilibrium adsorption constant related to the affinity of binding sites (L·mg^{-1}), and q_m is the maximum amount of dye per unit weight of adsorbent for complete monolayer coverage (mg·g^{-1}).

The Freundlich adsorption isotherm model, which is an empirical equation used to describe heterogeneous adsorption systems, can be represented as follows:

$$q_e = K_F C_e^{1/n} \quad (5)$$

...where q_e and C_e are defined as above, K_F is the Freundlich constant representing the adsorption capacity (mg·g^{-1}), and n is the heterogeneity factor depicting the adsorption intensity. In most references, Freundlich adsorption Eq. (5) may also be expressed as Eq. (6):

$$\ln q_e = \ln K_F + 1/n \ln C_e \quad (6)$$

The adsorption of DY42 was performed by shaking 0.5 g of sorbent in 50 mL DY42 at 30ºC and pH 12. It is known that the Langmuir isotherm is used on the supposition that the surface of the adsorbent is a homogenous surface, whereas the Freundlich isotherm applies to the adsorption process on a heterogeneous surface. The isotherm parameters of Langmuir and Freundlich for

Table 3. Langmuir and Freundlich constants for the adsorption of DY42 onto B-TBAI.

Freundlich			Langmuir			
R^2	1/*n*	K_f	R^2	K_L (L·mg^{-1})	q_m (mg·g^{-1})	Temperature (ºC)
0.952	0.244	7.878	0.996	0.148	18.98	20
0.985	0.162	9.64	0.998	0.160	19.98	30
0.978	0.175	8.667	0.982	0.154	17.60	40
0.984	0.179	6.680	0.980	0.142	16.40	50
0.988	0.199	6.620	0.990	0.130	15.32	60

Table 4. Thermodynamic parameters for adsorption of DY42 onto B-TBAI.

ΔSº (KJ·mol^{-1}·k^{-1})	ΔHº (J·mol^{-1})	ΔGº (KJ·mol^{-1})	K_c	T (K)
53.2	12.74	-2.85	3.23	293
		-3.40	3.86	303
		-3.76	4.25	313
		-4.43	5.2	323
		-5.58	7.5	333

adsorption of DY42 onto B-TBAI from graphs of equations 4 and 6 are shown in Table 3. A value for 1/*n* below one indicates a normal Langmuir isotherm, while 1/*n* above one is indicative of cooperative adsorption [36, 37]. As seen from Table 3, the Langmuir model yields a somewhat better fit R^2 than the Freundlich model. The values of 1/n between 0.162-0.244 indicate favorable adsorption [36].

Thermodynamic Parameters

In any adsorption process, entropy consideration must be taken into account in order to determine what process will occur spontaneously. Values of thermodynamic parameters are the actual indicators for practical application of a process. The amount of dye adsorbed at equilibrium at different temperatures (20, 30, 40, and 50ºC) have been examined to obtain thermodynamic parameters for the adsorption system. The thermodynamic parameters, change in the standard free energy ($\Delta G°$), enthalpy ($\Delta H°$), and entropy ($\Delta S°$) associated with the adsorption process and these were determined using the following equations [39]:

$$\Delta G° = -RT \ln K_C \quad (7)$$

...where, $\Delta G°$ is the standard free energy change, R the universal gas constant (8.314 J·mol^{-1}·K^{-1}), T the absolute temperature, and K_C the equilibrium constant. The apparent equilibrium constant of sorption K_C is obtained from:

$$K_C = C_A/C_S \quad (8)$$

...where K_C is the equilibrium constant, C_A is the amount of dye adsorbed on the adsorbent of solution at equilibrium (mg·L^{-1}), C_S is the equilibrium concentration of dye in the solution (mg·L^{-1}). K_C values were calculated at different temperature to allow the determination of the thermodynamic equilibrium constant (K_C) [38, 39]. The free energy changes also are calculated by using the following equation:

$$\ln K_C = -\Delta G°/RT = -\Delta H°/RT + \Delta S°/R \quad (9)$$

$\Delta H°$ and $\Delta S°$ calculate the slope and intercept of van't Hoff plots of ln K_C versus 1/T (Fig. 12). The results of thermodynamic parameters of DY42 adsorption onto B-TBAI are given in Table 4. The positive $\Delta H°$ value obtained in Table 4 indicates that the process is endothermic in nature. The overall standard free energy change during the adsorption process was negative for the experimental range of temperatures corresponding to a spontaneous physical process of DY42 adsorption, and the system did not gain energy from an external source. It becomes more favorable with increased temperature [19, 40].

Conclusion

The adsorption of DY42 from aqueous solution using organo-bentonite (B/TBAI) was investigated under different experimental conditions in batch process. The Langmuir adsorption isotherm was found to have the best fit to the experimental data. The adsorption kinetics can be predicted by pseudo-second-order kinetics. The results indicate that organo-bentonite (B/TBAI) is suitable as adsorbent material and it can be used as a cost-effective adsorbent for adsorption of DY42 from aqueous solutions.

References

1. AHIN S.S., DEMIR C., GUC S. Simultaneous UV-Vis spectrophotometric determination of disperse dyes in textile wastewater by partial least squares and principal component regression, Dyes Pigments **73**, 368, **2007**.

2. GOLOB V., OJSTRSEK A. Removal of vat and disperse dyes from residual pad liquors, Dyes Pigments **64**, 57, **2005**.
3. KIM T.H., PARK C., YANG J., KIM S. Comparison of disperse and reactive dye removals by chemical coagulation and Fenton oxidation, J. Hazard. Mater. **12**, 95, **2004**.
4. FOO K.Y., HAMEED B.H. Microwave-assisted preparation of oil palm fiber activated carbon for methylene blue adsorption, Chem. Eng. J. **66**, 792, **2011**.
5. NASUHA N., HAMEED B.H. Adsorption of methylene blue from aqueous solution onto NaOH-modified rejected tea, Chem. Eng. J. **166**, 783, **2011**.
6. ALBADARIN A.B., MANGWANDI C.M., AL-MUHTASEB A.H., WALKER G. M., ALLEN S., AHMAD M.N. M. Kinetic and thermodynamics of chromium ions adsorption onto low-cost dolomite adsorbent, Chem. Eng. J, **179**, 193, **2012**.
7. SALAMN J.M., NJOKU V.O., HAMEED B.H. Adsorption of pesticides from aqueous solution onto banana stalk activated carbon, Chem. Eng. J, **174**, 41, **2011**.
8. HAMEED B.H., AHMAD A.A., AZIZ N. Isotherms, kinetics and thermodynamics of acid dye adsorption on activated palm ash, Chem. Eng. J. **133**, (1-3), 195, **2007**.
9. SIRIANUNTAPIBOON S., SIRSONSAK P. Removal of disperse dyes from textile wastewater using bio-sludge, Bioreso. Technol. **98**, (5), 1057, **2007**.
10. NOUREDDINE B., SAMIR Q., ALI A. Adsorption of disperse blue SBL dye by synthesized poorly crystalline hydroxyl apatite, J. Environ. Sci. **20**, 1268, **2008**.
11. HASHEMIAN S. $MnFe_2O_4$/bentonite nano composite as a novel magnetic material for adsorption of acid red 138, African J. Biotechnol. **9**, (50), 8667, **2010**.
12. GUPTA G. S., PRASAD G., PANDAY K. K., SINGH V.N. Removal of chrome dye from dye aqueous solutions by fly ash, Water Air Soil Pollut. **37**, 13, **1988**.
13. HO Y. S., MCKAY G. Sorption of dye from aqueous solution by peat, J. Chem. Eng, **70**, 115, **1998**.
14. FERREERO F. Dye removal by low cost adsorbents: hazelnut shells in comparison with wood sawdust, J. Colloid. Interf. Sci. **142**, 144, **2007**.
15. HASHEMIAN S., SALIMI M. Nano composite a potential low cost adsorbent for removal of cyanine acid, Chem. Eng. J. **188**, 57, **2012**.
16. NAMASIVAYAM C., KAVITHA D. Removal of Congo red from water by adsorption onto activated carbon prepared from coir pith, an agricultural solid waste, Dyes Pigments, **54**, 47, **2002**.
17. ALLEN S.J., MCKAY G., KHADER K.Y.H. Equilibrium adsorption isotherms for basic dyes onto lignite, J. Chem. Tech. Biotechnol, **45**, 291, **1989**.
18. KANG Q., ZHOU W., LI Q., GAO B., FAN J., SHEN D. Adsorption of anionic dyes on poly(epichlorohydrin dimethyamine) modified bentonite in single and mixed dye solution, Appl. Clay. Sci. **45**, 280, **2009**.
19. SAFA OZCAN A., ERDEM B., OZCAN A. Adsorption of acid blue 193 from aqueous solutions onto Na-bentonite and DTMA-bentonite, J. Coll. Inter.Sci. **280**, 44, **2004**.
20. BOUBERKA Z., KACHA S. Sorption of an acid dye from aqueous solutions using modified clays, J. Hazrad. Mater. **B119**, 117, **2005**.
21. BASKARALINGAM P., PULIKESI M., ELANGO D., RAMAURTHI V., SIVANESAN S. Adsorption of acid dye onto organobentonite, J. Hazrad. Mater. **128**, (2-3), 138, **2006**.
22. YILMAZ N., YAPAR S. Adsorption properties of tetradecyl- and hexadexcyl trimethylammonium bentonites, Appl. Clay. Sci. **27**, 223, **2004**.
23. SHAKIR K., GHONEIMY H.F., ELKAFRAWY A.F., BEHEIR SH.G., REFAAT M. Removal of catechol from aqueous solutions by adsorption onto organophilic-bentonite, J. Hazar. Mater. **150**, 765, **2008**.
24. HASHEMIAN S. Study of adsorption of acid dye from aqueous solutions using bentonite, Main Group Chemistry, **6**, 97, **2007**.
25. MA J., CUI B., DAI J., LI D. Mechanism of adsorption of anionic dye from aqueous solutions onto organobentonite, J. Hazrad. Mater. **186**, (2-3), 1758, **2011**.
26. HASHEMIAN S. Removal of Acid Red 151 from water by adsorption onto nano-composite $MnFe_2O_4$/kaolin, Main Group Chem. **10**, 105, **2011**.
27. KHENIFI A., ZHRA B., KAHINA B., HOUARI H., ZOUBIR D. Removal of 2, 4- DCP from wastewater by CTAB/bentonite using one–step two-step methods: A comparative study, Chem. Eng. J. **146**, 345, **2009**.
28. BOUBERKA Z., KHENIFI A., AIT MAHMED H., HADDOU B., BELKAID N., BETTAHAR N., DERRICHE Z. Adsorption of supranol yellow 4GL from aqueous solution by surfactant-treated aluminum/chromium-intercalated bentonite, J. Hazard. Mater. **162**, 378, **2009**.
29. AKCAY M. Characterization and determination of the thermodynamic and kinetic properties of p-CP adsorption onto organophilic bentonite from aqueous solutions. J. Colloid Interface Sci. **280**, 299, **2004**.
30. EREN E., AFSIN B. An investigation of Cu (II) adsorption by raw and acid –activated bentonite: A combined potentiometric, thermodynamic, XRD, IR, DTA study, J. Hazard. Mater. **151**, 682, **2008**.
31. JIAN J.Q., COOPER C., ZOUKI S. Comparison of modified montmorillonite adsorbents: part I. Preparation, characterization and phenol adsorption. Chemosphere **47**, 711, **2002**.
32. YILMAZ N., YAPAR S. Adsorption properties of tetradecyl-and hexadecyl trimethylammonium bentonite, Appl. Clay Sci. **27**, 223, **2004**.
33. LATAYE, D.H., MISHRA I.M., MALL I.D., Adsorption of 2-picolinine onto bagasse fly ash from aqueous solution, Chem. Eng. J. **138**, 35, **2008**.
34. BULUT Y., AYDIN H. A kinetic and thermodynamics study of methylene blue adsorption on wheat shells, Desalination, **194**, 259, **2006**.
35. OFOMAJA A.F. Kinetic study and sorption mechanism of methylene blue and methyl violet onto mansonia wood sawdust, Chem. Eng. J. **143**, 85, **2008**.
36. HAMEED B.H., DIN A.T.M., AHMAD A. L. Adsorption of methylene blue onto bamboo-based activated carbon, J. Hazard. Mater. **141**, (3), 819, **2007**.
37. OVICIC J., MILUTIONOVIC-NIKOLIC N., GRZETIC A., JOVAOVIC I. Orgaobentonite as a efficient textile dye sorbent, Chem. Eng.Technol. **31**, (4), 567, **2008**.
38. BULUT Y., AYDIN H. A kinetic and thermodynamics study of methylene blue adsorption on wheat shells, Desalination, **194**, 259, **2006**.
39. DOGAN M., ALKAN M.A., TÛRKYILMAZ Y. Kinetics and mechanism of removal of methylene blue by adsorption onto perlite, J. Hazard. Mater. **B109**, 141, **2004**.
40. ATIA A. A. Adsorption of chromate and molybdate by cetylpridinium bentonite, Appl. Caly Sci. **41**, 73, **2008**.